Macromolecules

Article

pubs.acs.org/Macromolecules

Surface Properties of Bottlebrush Polymer Thin Films

Xianyu Li, Stacy L. Prukop, Sibani Lisa Biswal, and Rafael Verduzco*

Department of Chemical and Biomolecular Engineering, Rice University, 6100 Main Street, Houston, Texas 77005, United States

Supporting Information

ABSTRACT: Bottlebrush polymer thin films may be attractive for the preparation of antifouling and/or stimuli-responsive surface coatings due to the high grafting density and conformational flexibility of polymeric side chains, but bottlebrush polymer thin films have not been previously reported and their surface properties are unknown. Herein, we report a study of the surface properties of mixed bottlebrush polymer (MBBPs) films. MBBPs with hydrophobic polystyrene (PS) and hydrophilic poly(ethylene glycol) (PEG) side chains are synthesized using a "grafting-through" ring-opening metathesis polymerization (ROMP) approach. Stimuli-responsive MBBPs films are prepared by spin-casting a solution of MBBPs onto a solid surface, and the resulting film morphology and surface properties are characterized using atomic force microscopy (AFM), grazing-incidence small-angle X-ray scattering (GISAXS), water contact angle measurements, and X-ray photoelectron spectroscopy (XPS). The water contact angles of MBBPs films decrease or increase upon exposure of the MBBPs films to selective solvents methanol or cyclohexane, respectively. This contact angle change is dependent on the length of the PEG side chain; longer PEG side chains result in greater contact angle changes with solvent exposure. Consistent with water-contact angle measurements, XPS indicates enrichment of PEG or PS chains at the film surface after exposure of the MBBPs film to methanol or cyclohexane solvent vapors, respectively. Finally, it is demonstrated that bottlebrush polymer films can be stabilized by the addition of a radical cross-linker and irradiation with UV light. This work demonstrates that bottlebrush polymers enable the preparation of stimuli-responsive, "brush-like" polymeric coatings using simple solution processing methods.

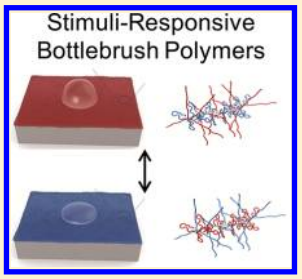

INTRODUCTION

Bottlebrush polymers are macromolecules with polymeric side chains on each repeat unit (Figure 1). The dense grafting of polymeric side chains results in both backbone and side-chain extension,[1−4] giving rise to large, highly extended macromolecules with individual molecules exceeding 100 nm in backbone length in some cases.[5] As a result of their size and novel structure, bottlebrush polymers are candidates for a number of applications, including rheological modifiers,[6] polymeric photonics,[7] and nanoparticles for drug delivery.[8−10] While thin films of bottlebrush polymers can be easily prepared using common solvent-based techniques including spin-coating, dip-coating, and inkjet printing, bottlebrush polymer thin films have not been previously reported and their surface properties are unknown. Because of the high grafting density and conformational flexibility of the side chains, such coatings may be attractive for the preparation of antifouling and/or stimuli-responsive surfaces.

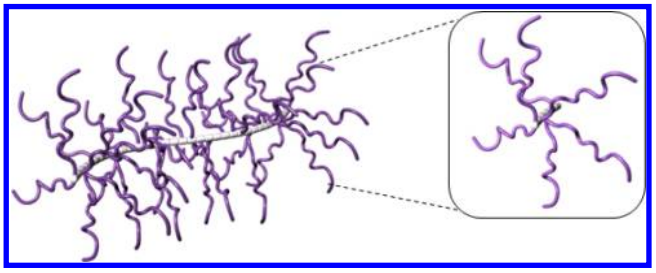

Figure 1. Schematic for a single bottlebrush molecule. Every repeat unit on the polymer backbone has a polymeric side chain attached, and steric interactions between the side chains results in backbone and side-chain stretching.

Bottlebrush polymer thin films may exhibit surface properties characteristic of polymer brush films, which are comprised of polymer chains densely tethered to a surface.[11] Steric interactions in polymer brush films result in chain stretching normal to the surface and give rise to novel and potentially useful surface properties. These types of films are currently of interest for the preparation of nontoxic antifouling surfaces,[12,13] self-cleaning surfaces,[14] stimuli-responsive surfaces,[15−17] organic electronics,[18,19] and other applications.[20,21] However, the use of polymer brush films for some applications may be impractical. Polymer brush films are commonly prepared through surface initiated polymerizations[22,23] which require a functionalized, reactive surface as well as polymerization under inert conditions. Accomplishing this over a large surfaces, such as a ship's hull for antifouling films, would be costly and technically difficult. Bottlebrush polymers provide a potential alternative and they can be easily applied over any surface using solution processing techniques such as inkjet printing, dip coating, or spray coating.

In analogy to the switchable wettability that has been observed in polymer brush films,[24−28] bottlebrush polymers with mixed hydrophobic and hydrophilic side chains may show switchable surface properties on exposure to solvents that

Received: May 22, 2012
Revised: August 9, 2012
Published: August 20, 2012

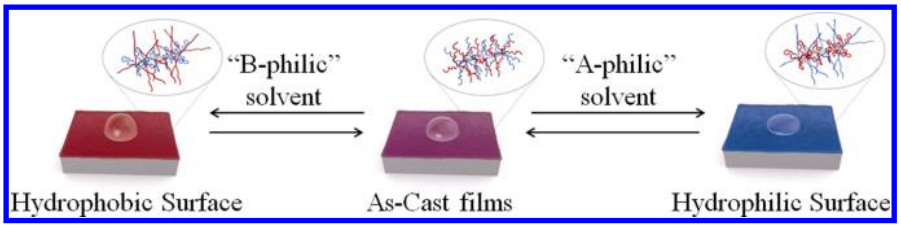

Figure 2. Schematic for a bottlebrush polymer films with reversible wettability. The schematic shows a film of mixed bottlebrush polymers, which have both hydrophilic and hydrophobic side chains. Exposure to a selective solvent for one side chain will result in enrichment of those chains at the film surface and lead to an increase or decrease in the water contact angle.

selective for one of the chains (Figure 2). For a mixed bottlebrush polymer film with hydrophobic polystyrene (PS) and hydrophilic poly(ethylene glycol) (PEG) side chains, exposure to cyclohexane (which is selective for PS) may result in enrichment of PS chains at the film surface and an increase of the water contact angle. On the other hand, exposure of the film to methanol (which is selective to PEG) may result in enrichment of PEG chains at the film surface and a decrease in the water contact angle. The length of the side chains may also play a role. Short side chains may have little conformational flexibility, while longer side chains are expected to have more conformational flexibility, potentially resulting in larger contact angle changes with solvent exposure. The goal of this study is to characterize the surface properties of bottlebrush polymer thin films and, in particular, determine if bottlebrush polymer films show stimuli-responsive surface properties.

Experimental verification of switchable wettability requires the preparation of mixed bottlebrush polymers (MBBPs) which have distinct polymeric side chains connected to a polymeric backbone. Three general approaches for synthesizing bottlebrush polymers include "grafting-to", "grafting-from", and "grafting-through".[29] Each strategy has particular advantages and disadvantages, but the "grafting-from" approach has been the most popular method for making bottlebrush polymers,[30−33] including the preparation bottlebrush polymers with block copolymer side chains as well as nanocapsules with hollow interiors.[10,34−39] However, the "grafting-through" approach, which involves the polymerization of reactive macromonomers, is the only method which guarantees uniform side chains attached to each repeat unit. Early studies on bottlebrush polymers relied on a "grafting-through" approach, but this generally resulted in polymers with a low degree of polymerization and broad polydispersities.[40−45] Recently, an efficient "grafting-through" scheme for synthesizing bottlebrush polymers based on ring-opening metathesis polymerization (ROMP) has been developed.[46−49] Bowden and co-workers demonstrated in 2004 that ROMP was an effective approach for polymerizing macromonomers terminated with a norbornyl group.[47] Subsequently, Grubbs and co-workers showed that using a more reactive modified second- or third-generation Grubbs catalyst enabled control over the length and polydispersity of molecular brushes. Their approach enabled the preparation of molecular brushes with complex structures, such as random and "blocky" molecular brush copolymers.[9,46,49,50]

Herein, we report a study of the surface properties of mixed bottlebrush polymer (MBBPs) films. Well-defined MBBPs are prepared through a "grafting-through" ROMP approach using a mixture of PEG and PS macromonomers. Gel-permeation chromatography (GPC) and ^{1}H NMR show that well-defined MBBPs with >90% conversion of the macromonomers can be prepared by ROMP. MBBPs films are prepared by spin-casting a solution of MBBPs onto a solid surface, and the resulting surface properties are characterized by AFM, contact angle, GISAXS, and XPS measurements. The water contact angle and composition of the top film can be modified by exposing the MBBPs film to methanol or cyclohexane vapors, which are selective to PEG or PS side chains, respectively. Furthermore, it is demonstrated that bottlebrush polymers films can be stabilized by the addition of a bifunctional radical cross-linker. This work demonstrates that bottlebrush polymers enable the preparation of stimuli-responsive, "brush-like" polymeric coatings using simple and economically viable solution processing methods.

RESULTS AND DISCUSSION

Synthesis of Bottlebrush Polymers. Mixed bottlebrush polymers were prepared via a "grafting-through" synthetic approach that relies on ROMP of ω-norbornenyl macromonomers using a highly active, modified second-generation Grubb's catalyst. This synthetic approach ensures that each repeat unit has a side chain attached and can be used to prepare bottlebrush polymers with controlled side chain and backbone length as well as low polydispersity.[46,49] PEG macromonomers were prepared by coupling azide-terminated PEG (purchased from Nanocs) to alkynyl-terminated *exo*-norbornene though a copper-catalyzed azide−alkyne "click" coupling reaction (Scheme 1, top). PS macromonomers were prepared via reversible addition−fragmentation chain transfer (RAFT) from an *exo*-norbornene-functionalized chain-transfer agent (CTA) (Scheme 1, bottom). Two different molecular weights for each macromonomer (summarized in Table 1) were prepared and used in the synthesis of bottlebrush polymers.

Scheme 1. Synthetic Scheme for the Preparation of ω-Norbornenyl Poly(ethylene glycol) (NB-PEG) (top) and Polystyrene (NB-PS) (bottom) Macromonomers

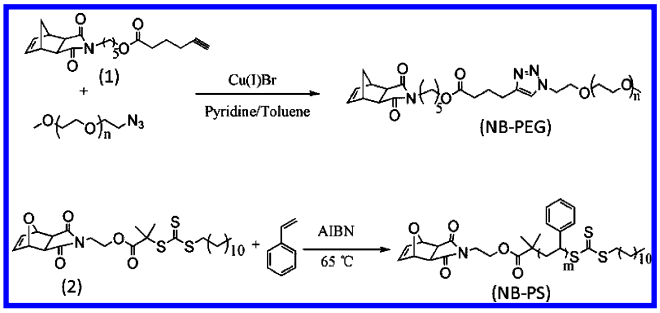

^{1}H NMR provides evidence of quantitative end-group control for both macromonomers. In the case of NB-PEG5K (Figure 3, top), protons corresponding to the terminal

dx.doi.org/10.1021/ma301046n | *Macromolecules* 2012, 45, 7118−7127

Table 1. Characteristics of Norbornene-Functionalized Macromonomers

macromonomer[a]	polymer	$M_{w,GPC}$[b] (kg/mol)	DP_{GPC}[c]	DP_{NMR}[d]	PDI[b]
NB-PS3K	polystyrene	3400	28	34	1.18
NB-PS6K	polystyrene	6600	55	61	1.14
NB-PEG2K	poly(ethylene glycol)	2300	48	55	1.09
NB-PEG5K	poly(ethylene glycol)	5600	125	120	1.02

[a]The sample name reflects the type and molecular weight of the polymer. [b]M_w is measured by GPC relative to monodisperse PS standards. [c]Number-averaged degree of polymerization (DP) calculated based on the GPC estimate of $M_n = M_w/PDI$. [d]The NMR estimate for DP is calculated by comparing the integrated intensity for H in the polymer backbone to that for H in the norbornene end group.

norbornene as well as the proton on the triazole ring are clearly resolved by ^{1}H NMR. NB-PEG2K shows similar features. For the polystyrene macromonomer NB-PS6K (Figure 3, bottom), peaks corresponding to the norbornene end group and the trithiocarbonate functionality are clearly resolved by ^{1}H NMR, and similar features are observed for NB-PS3K. Calculations of polymer molecular weights using ^{1}H NMR integrated intensities are in good agreement with the estimate provided by GPC for all polymers, indicating good control over the polymer end group. The polydispersity (PDI) of all macromonomers is less than 1.2 (Table 1).

MBBPs were synthesized via ROMP of ω-norbornenyl macromonomers (Scheme 2). GPC with refractive index (RI) and multiangle laser light scattering (MALLS) detection was used to monitor the reaction and provide a quantitative measure of conversion and bottlebrush polymer molecular weight and polydispersity (see Figure 4 and Supporting Information Figures S2 and S3). ^{1}H NMR was used to monitor the conversion of the *exo*-norbornene end group to a poly(norbornene) or poly(oxanorbornene) backbone (see Supporting Information Figure S4). The content of PS and PEG side chains in the MBBPs is determined by comparing the ^{1}H NMR integrated intensities corresponding to each side chain. The molar ratio of PS to PEG macromonomers was 1:1 for all MBBPs except for P(NB-PS3K-*m*-NB-PEG2K)-2, for which the ratio was 2:1. This latter sample was prepared due to the difficultly in extracting a reliable water contact angle for P(NB-PS3K-*m*-NB-PEG2K)-1 films, as described below.

As demonstrated in Table 2, the ROMP-based "grafting-through" approach is effective for preparing a series of well-defined MBBPs with systematically varying side-chain lengths and composition. In a typical polymerization reaction, conversion of the macromonomers was >90%. The MBBPs have backbone DPs ranging from 30 to 60 (corresponding to total molecular weights of 100−300 kg/mol) and relatively low polydispersities (~1.2 or lower) for most samples prepared. Finally, ^{1}H NMR indicates complete conversion of the *exo*-norbornene functionality to a poly(norbornene) or poly(oxanorbornene) backbone and proves incorporation of both PS and PEG side chains into the bottlebrush polymers.

Preparation of Bottlebrush Polymer Thin Films. Bottlebrush polymer thin films can be prepared by spin-casting a dilute solution of MBBPs onto a surface. ITO was used for all surface property measurements; MBBPs films were found to be unstable on silicon and tended to dewet, as has been noted for PS films.[51] Smooth films can be achieved on ITO by spin-casting a sufficiently thick (100 nm or greater) polymer film. The film thickness and surface coverage depend on the concentration used for spin-coating; for this study, all films are

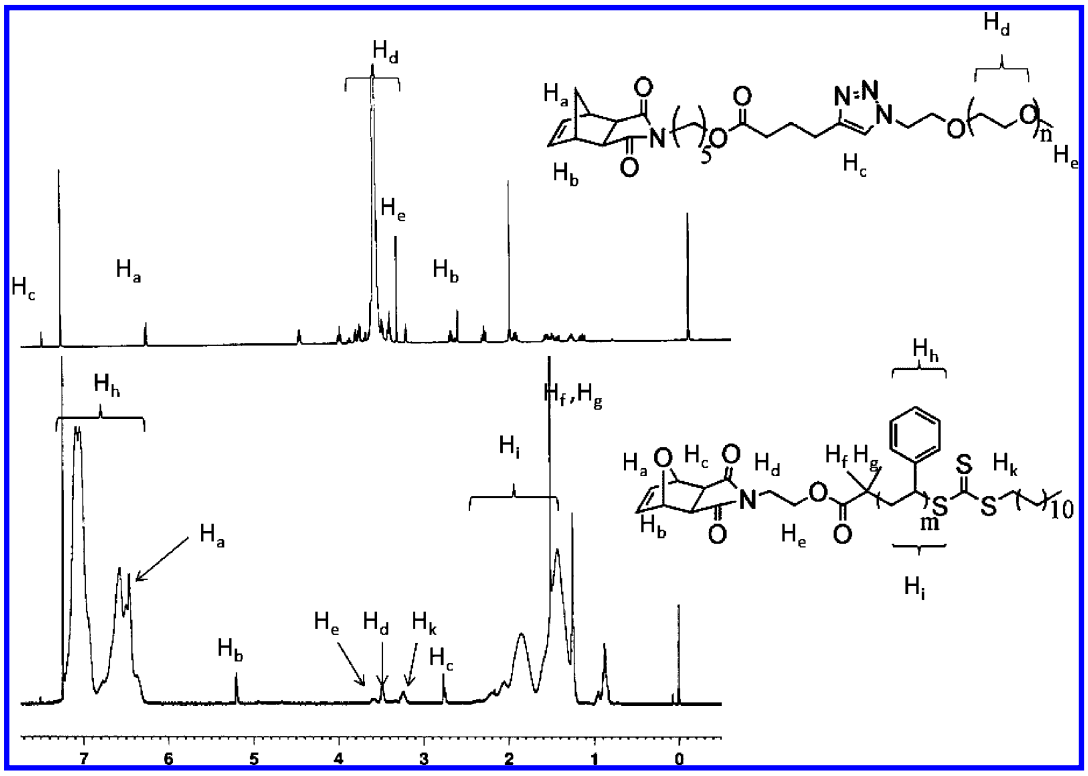

Figure 3. ^{1}H NMR spectrum for macromonomers NB-PEG5K (top) and NB-PS6K (bottom).

dx.doi.org/10.1021/ma301046n | *Macromolecules* 2012, 45, 7118−7127

Scheme 2. Mixed Bottlebrush Polymers (MBBPs) Are Prepared via ROMP of NB-PS and NB-PEG Macromonomers, Resulting in Bottlebrush Polymers with Mixed Hydrophobic and Hydrophilic Side Chains

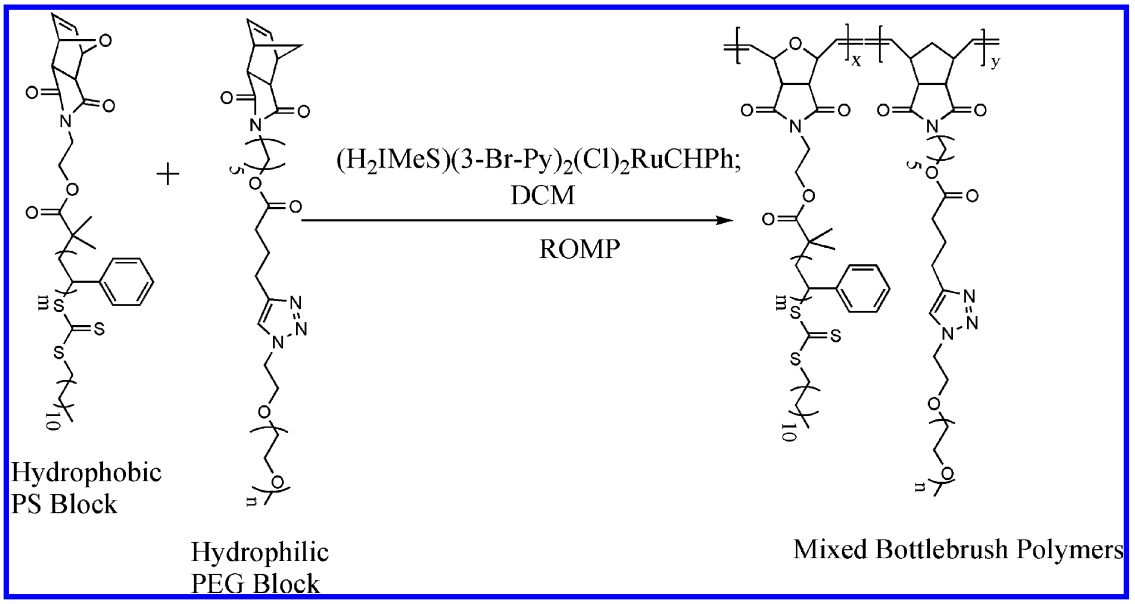

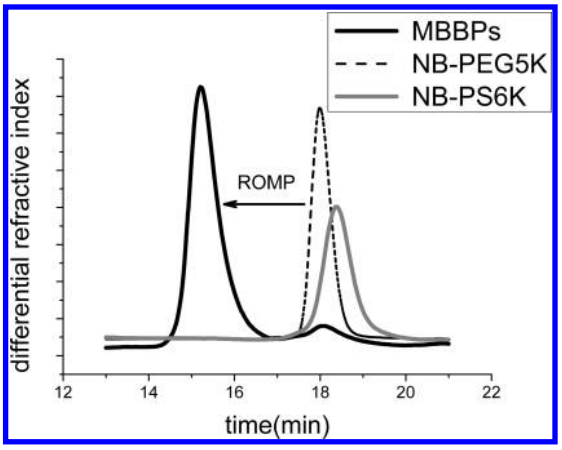

Figure 4. GPC traces for MBBPs P(NB-PS6K-*m*-NB-PEG5K) (black line) and corresponding NB-PS6K (dashed line) and NB-PEG5K (gray line) macromonomers. The GPC shows a clear shift in the molecular weight after ROMP as well as some residual (<5 wt %) macromonomer.

spin-cast at 1500 rpm/s for 30 s and then at 500 rpm/s for an additional 30 s. Spin-casting a 20 mg/mL solution of MBBPs in chloroform results in a smooth film with complete surface coverage (see Figure 5 and Supporting Information Figure S5). MBBPs films appear uniform by visual inspection and under optical microscopy, and AFM indicates that the surface roughness is ∼5 nm (see Supporting Information Figure S6). On the other hand, when a dilute (1 mg/mL) chloroform solution is used, surface coverage is incomplete and individual polymers can be imaged by AFM (Figure 5b, right). For P(NB-PS6K-*m*-NB-PEG5K), individual bottlebrush polymers are cylindrical in shape have a length of 40−50 nm. This size is reasonable based on the DP of 51 measured by GPC and assuming a backbone step length l_m of 0.25 nm.[5] For a fully stretched backbone, the bottlebrush polymer length would be ∼64 nm while a Gaussian chain with the same step length and DP would be just 9 nm in size. Thus, MBBPs are highly stretched due to steric interactions between the polymeric side chains.

Uniform MBBPs films exposed to methanol and/or cyclohexane vapor in a sealed annealing chamber showed no

Table 2. Characteristics of Bottlebrush Polymers Prepared for This Study

samples[a]	M_w[b] (kg/mol)	DP_{GPC}	PDI	conv[c]	PEG content[d] (mol %)	PEG content[d] (mass %)
P(NB-PS6K-*m*-NB-PEG5K)	307	51	1.13	95	52.5	48.0
P(NB-PS6K-*m*-NB-PEG2K)	302	67	1.17	93	52.5	30.0
P(NB-PS3K-*m*-NB-PEG2K)-1	165	66	1.22	91	50.6	41.7
P(NB-PS3K-*m*-NB-PEG2K)-2	93.2	35	1.38	94	39.6	30.4
P(NB-PS3K-*m*-NB-PEG5K)	132	33	1.15	97	50.6	63.1
P(NB-PS6K)	207	35	1.79	96	0.00	0.00
P(NB-PS3K)	68.7	20	1.02	96	0.00	0.00
P(NB-PEG2K)	59.6	30	1.07	93	100	100
P(NB-PEG5K)	195	35	1.11	90	100	100

[a]The sample name reflects the molecular weight and type of side chains in the MBBPs. All samples that involve two different side chains are mixed bottlebrush polymers with a molar ratio of 1:1, except for P(NB-PS3K-*m*-NB-PEG2K)-2, which was prepared with a 2:1 molar ratio of PS3K to PEG2K. [b]M_w determined by GPC with MALLS analysis. [c]Conversion of the macromonomers after ROMP polymerization are calculated using GPC with RI detection by comparing the peak area of MBBPs to the peak area of residual macromonomers. [d]The final ratio of PEG to PS is calculated by comparing the ^{1}H NMR integrated intensities corresponding to each side chain.

dx.doi.org/10.1021/ma301046n | *Macromolecules* 2012, 45, 7118−7127

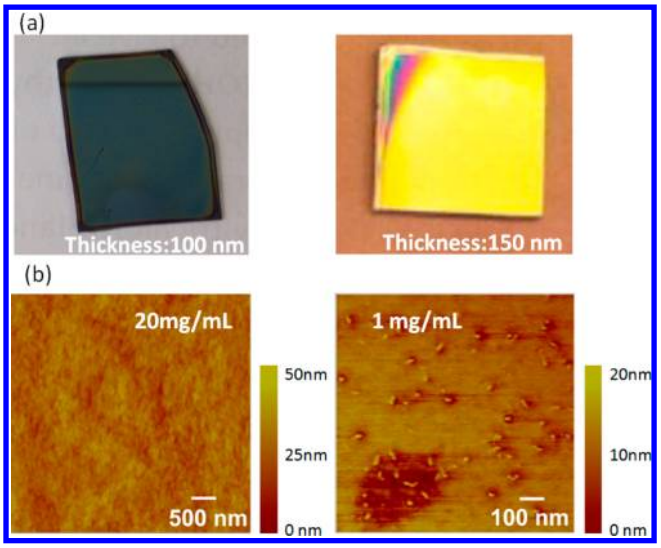

Figure 5. Representative images of P(NB-PS6K-*m*-NB-PEG5K) films on silicon (a) and AFM height images for MBBP films on ITO prepared via spin-casting using different concentrations (b). Films shown in (a) were prepared on silicon to allow for visualization from a reflective surface, but all surface property measurements reported are for films on ITO. The images in (a) demonstrate that uniform films can be prepared on a surface by spin-casting, and the surfaces are ∼2 cm across. AFM images (b) show a film with uniform coverage when a 20 mg/mL solution is used, but at lower MBBPs concentrations (1 mg/mL) surface coverage is incomplete and individual polymers can be resolved.

significant changes to film uniformity after solvent treatment. AFM analysis of surfaces before and after solvent treatment (see Supporting Information Figure S6) indicates that film roughness increases slightly (from 5 to 10 nm) for both methanol and cyclohexane vapor treatments. No microphase-separated structure was observed in any MBBPs film. This was verified by both AFM and GISAXS measurements (see Supporting Information Figure S7). While self-organization has been reported previously in bottlebrush polymer melts,[52,53] the lack of any self-assembly for the present materials may be due to the film thickness chosen or the relatively short length of the side chains in the MBBPs studied.

Surface Properties of Bottlebrush Polymer Thin Films. Bottlebrush polymer thin films are prepared by spin-casting a solution of bottlebrush polymer in a good solvent (chloroform) for both side chains. Subsequent treatment by selective solvents may preferentially swell either the PEG or PS side chains, leading to a measurable change in the surface composition and water contact angle. This responsiveness with solvent treatment may also depend on the length of the side chains. Solvent-dependent stimuli-responsive properties have been reported for polymer brush films[24−28] but not for bottlebrush polymer films.

Bottlebrush polymer films were prepared on clean ITO-coated glass from a 20 mg/mL solution in chloroform. For comparison to MBBPs films, contact angles were also measured for ITO-coated glass, NB-PS6K and NB-PEG2K macromonomers, and P(NB-PS6K) and P(NB-PEG2K) bottlebrush polymers (Figure 6 and Table 3). Clean ITO is a hydrophilic surface on which water completely wets the surface. The water contact angles are higher for polymeric thin film coatings, and the water-contact angles were significantly higher for bottlebrush polymer films compared with corresponding macromonomer films (Table 3). NB-PEG2K has a water contact angle of 35°, and P(NB-PEG2K) films have a much higher contact angle (∼80°). As expected, NB-PS6K macromonomer films have a larger contact angle than NB-PEG2K films, with a contact angle of ∼90°, while P(NB-PS6K) films have an even larger contact angle of 102°. MBBPs films have water contact angles that range between those for the macromonomers and bottlebrush polymers, although all have a contact angle greater than 60°. The contact angles measured for bottlebrush polymer and mixed bottlebrush polymer films are consistent with previous measurements on PS and PEG brush films. A variety of polystyrene brush films have been reported with contact angles in the range of 90°−100°.[28,54−57] A broader range of values has been reported for PEG brushes and self-assembled monolayers (SAMs). PEG brush films have contact angles reported ranging from 30° to 70°, depending on the surface coverage, PEG length, and preparation method.[58−60] SAMs of oligo-ethylene glycol show a contact angle of roughly 68°,[61] while star-shaped PEG surfaces show a contact angle of 64°.[62]

To test the conformational flexibility of the side chains, bottlebrush polymer films were exposed to a selective solvent (methanol or cyclohexane) and subsequently dried under vacuum overnight before measurement. Cyclohexane is a theta solvent for PS (at 34.5 °C) but a poor solvent for PEG, and treatment with cyclohexane vapor is thus expected to result in selective swelling and enrichment of NB-PS chains at the air−film interface. Methanol, on the other hand, is a good solvent for PEG but poor solvent for PS, and therefore treatment with methanol vapor is expected to result in swelling and enrichment of NB-PEG side chains at the air−film surface. This is shown schematically in Figure 2, where treatment with a selective solvent results in a change in side-chain conformation and surface wettability.

The measured water contact angles changed for all MBBPs films with solvent treatment, with methanol-treated surfaces exhibiting a decrease in contact angle and cyclohexane-treated surface exhibiting an increase in contact angle relative to as-cast films (see Table 3 and Figure 7). Furthermore, MBBPs with longer PEG side chains exhibit larger contact angle changes.

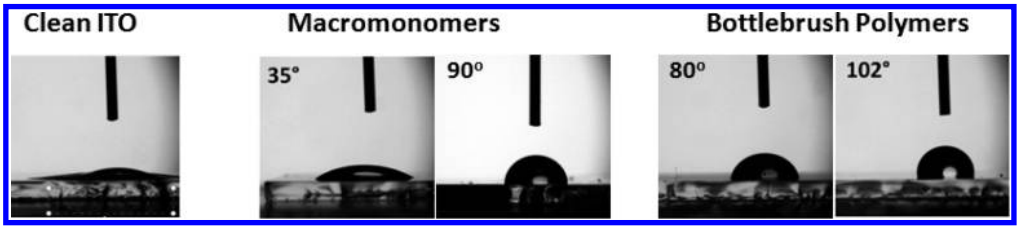

Figure 6. Micrographs of water droplets on clean ITO and polymer-coated ITO surfaces. From left to right: clean ITO, NB-PEG2K, NB-PS6K, P(NB-PEG2K), and P(NB-PS6K). Clean ITO and NB-PEG films are hydrophilic, but all other polymeric films are more hydrophobic.

dx.doi.org/10.1021/ma301046n | *Macromolecules* 2012, 45, 7118−7127

Table 3. Water Contact Angles for As-Cast and Solvent-Annealed Polymer Films

polymer sample	polymer type	contact angle (deg)	methanol treated (deg)	cyclohexane treated (deg)
blank ITO	N/A	(fully spread)		
NB-PEG2K	macromonomer	35.0 ± 0.5		
NB-PS6K	macromonomer	90.4 ± 0.2		
P(NB-PEG2K)	bottlebrush	79.5 ± 0.7		
P(NB-PS6K)	bottlebrush	102 ± 0.3		
P(NB-PS6K-*m*-NB-PEG5K)	mixed bottlebrush	69.6 ± 0.4	63.8 ± 0.8	72.5 ± 0.6
P(NB-PS6K-*m*-NB-PEG2K)	mixed bottlebrush	73.0 ± 0.6	71.1 ± 0.4	74.8 ± 0.3
P(NB-PS3K-*m*-NB-PEG2K)-1	mixed bottlebrush	69.3 ± 0.7	N/A	N/A
P(NB-PS3K-*m*-NB-PEG2K)-2	mixed bottlebrush	75.4 ± 0.3	72.0 ± 0.6	77.0 ± 0.5
P(NB-PS3K-*m*-NB-PEG5K)	mixed bottlebrush	53.6 ± 0.3	46.8 ± 1.3	58.3 ± 0.7

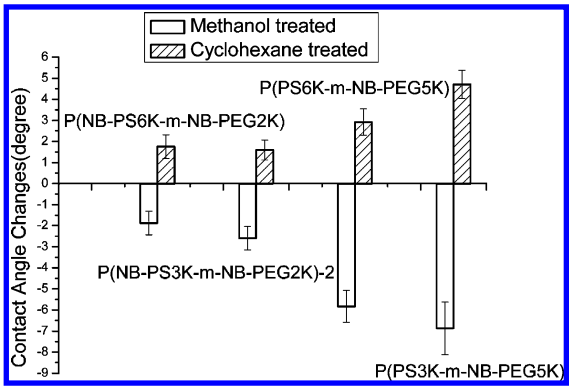

Figure 7. Changes in water contact angles for MBBPs films exposed to either methanol or cyclohexane vapors.

For example, for P(NB-PS6K-*m*-NB-PEG5K) films have a contact angle of ~69.6° as-cast, and the contact angle increases by ~2.9° after cyclohexane vapor treatment but decreases by 5.8° after methanol vapor treatment. A larger change is seen for P(NB-PS3K-*m*-NB-PEG5K) with 6.8° and 4.7° contact angle changes with methanol and cyclohexane treatment, respectively. By comparison, MBBPs films with 3K NB-PS side chains showed a maximum change of only 3.4° for methanol and cyclohexane treatment. The water contact angle for P(NB-PS6K-*m*-NB-PEG2K) films changed by less than 2° with methanol and cyclohexane treatments. The relatively small change in contact angle for P(NB-PS6K-*m*-NB-PEG2K) may be due to the reduced flexibility of PS chains compared with PEG side chains. P(NB-PS3K-*m*-NB-PEG2K)-1 films were unstable under solvent treatment; instead, MBBPs films with the same side chains but a 2:1 ratio of NB-PS3K and NB-PEG2K side chains were studied (P(NB-PS3K-*m*-NB-PEG2K)-2). These films show similar contact angles and solvent responsiveness as P(NB-PS6K-*m*-NB-PEG2K), which might be expected due to the similar overall content of NB-PS and NB-PEG side chains in both MBBPs.

The contact angle measurements indicate that MBBPs films show stimuli-responsive behavior. For the materials studied, greater contact angle changes were detected for MBBPs with longer PEG side chains. This indicates that conformational flexibility of the side chains is important for the responsiveness of the films and that, for the MBBPs in the present study, the conformational flexibility of the hydrophilic side chain plays a more significant role in water contact angle changes.

Surface Chemistry of Bottlebrush Polymer Thin Films. XPS was used to quantify the chemical composition of the top MBBPs film surface. Films were prepared on clean ITO-coated glass substrates, and XPS measurements were carried out at an incidence angle of 45°. At this incidence angle, XPS measures the composition of roughly the top 5−10 nm of the polymer film and can provide direct evidence for changing composition near the top film surface, as shown in Figure 8 for P(NB-PS6K-*m*-NB-PEG5K) MBBPs films. For the as-cast P(NB-PS6K-*m*-NB-PEG5K) MBBPs film, the molar ratio of carbon to oxygen (C/O) on the surface is 8.5. The ratio increases to 13.3 after treatment with cyclohexane vapor but decreases to 6.5 after methanol vapor treatment. This indicates that solvent treatment does indeed change the composition of the MBBPs film at the film−air interface, resulting in a greater NB-PS content after cyclohexane treatment and a greater NB-PEG content after methanol treatment, consistent with contact angle measurements.

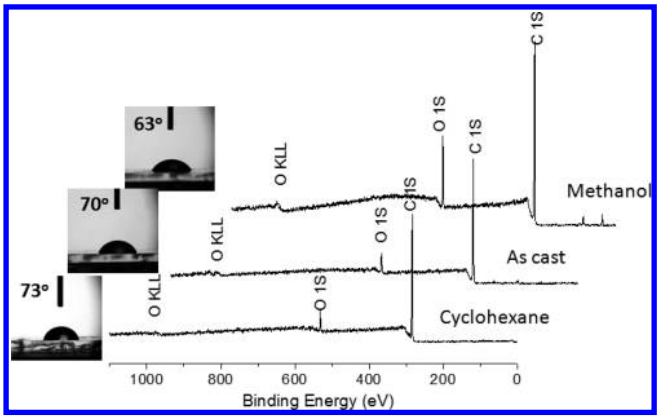

Figure 8. XPS spectra and corresponding contact angle images for P(NB-PS6K-*m*-NB-PEG5K) MBBPs films before and after solvent treatments.

All MBBPs films and P(NB-PS6K) and P(NB-PEG2K) bottlebrush polymer films were similarly measured by XPS. As shown in Table 4, the C/O ratio changes with solvent treatment for all MBBPs films and shows trends consistent with those expected from contact angle measurements. For example, a comparison of P(NB-PS6K-*m*-NB-PEG5K) with P(NB-PS6K-*m*-NB-PEG2K) films shows that the former have a lower C/O ratio and exhibit larger changes in the C/O ratio with solvent treatment. Furthermore, P(NB-PS3K-*m*-NB-PEG5K) films exhibit the lowest C/O ratio for all MBBPs studied, consistent with their relatively low contact angle. P(NB-PS3K-*m*-NB-PEG2K)-2 films show surprisingly large changes in the C/O ratio with solvent vapor treatment, but these MBBPs films still have a larger C/O ratio compared with P(NB-PS3K-*m*-NB-PEG5K) and P(NB-PS6K-*m*-NB-PEG5K) films.

dx.doi.org/10.1021/ma301046n | *Macromolecules* 2012, 45, 7118−7127

Table 4. XPS Results of MBBPs or HBBs[a]

sample polymers	C/O (as-cast)	C/O (methanol-treated)	C/O (cyclohexane-treated)
P(NB-PS6K-*m*-NB-PEG5K)	8.5	6.5 (−24%)	13.3 (+56%)
P(NB-PS6K-*m*-NB-PEG2K)	12.4	11.2 (−12%)	16.2 (+38%)
P(NB-PS3K-*m*-NB-PEG2K)-1	6.4	N/A	N/A
P(NB-PS3K-*m*-NB-PEG2K)-2	9.8	7.3 (−26%)	12.9 (+32%)
P(NB-PS3K-*m*-NB-PEG5K)	6.1	5.3 (−13%)	7.5 (+23%)
P(NB-PS6K)	27.5	N/A	N/A
P(NB-PEG2K)	3.3	N/A	N/A

[a]The C/O ratio is determined by taking a ratio of the C 1s and O 1s signals measured by XPS. The value in parentheses shows the percentage change in the C/O ratio relative to the as-cast value.

Cross-Linking and Stabilization of Bottlebrush Polymer Films. The long-term stability of bottlebrush polymer films is important for practical applications of MBBPs films, for example, for the development of nontoxic coatings to inhibit marine biofouling. The films described above were un-cross-linked and only physically adsorbed to the surface, but chemical cross-linking of MBBPs films is possible using bifunctional benzophenone chromophore bis-3-benzoyl benzoic acid ethylene glycol (Figure 9c).[51] To demonstrate film stabilization,

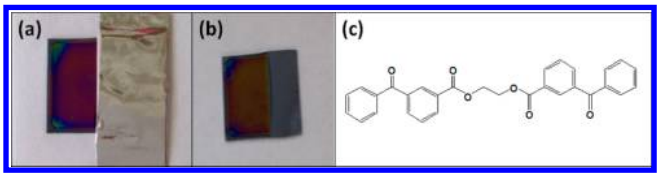

Figure 9. Cross-linked films before (a) and after (b) washing with THF and the chemical structure of the bifunctional benzophenone cross-linker used (c). Films shown in (a) and (b) were prepared on silicon to allow for visualization from a reflective surface.

P(NB-PS3K-*m*-NB-PEG2K)-1 was dissolved in chloroform (20 mg/mL), and the bifunctional, photoactive benzophenone cross-linker was added at a molar ratio of 1:100 relative to P(NB-PS3K-*m*-NB-PEG2K)-1. This MBBP was chosen for testing the effect of cross-linking on stability since it formed the least stable MBBPs film. The solution was spin-cast onto a clean silicon substrate, and half of the resulting MBBPs film was irradiated by UV light while the other half was protected from exposure using aluminum foil (Figure 9a). After immersing the film in THF, only the irradiated portion of the film remained while the nonirradiated portion fully dissolved and was removed from the surface. Irradiated films were also stable when immersed in water. This indicates that robust MBBPs films can be prepared by addition of a small amount of bifunctional benzophenone chromophore.

CONCLUSION

Well-defined mixed bottlebrush polymers (MBBPs) with targeted side chain and backbone molecular weight can be prepared via ROMP of ω-norbornenyl macromonomers, and uniform MBBPs thin films can be prepared by spin-casting a solution of MBBPs onto a surface. Stimuli-responsive surface properties in MBBPs thin films arise due to the conformational flexibility of the polymeric side chains and are analogous to what has been observed in polymer brush films, in which polymer chains are end-tethered to a surface. Treatment of MBBPs films with methanol vapor results in a more hydrophilic surface, while treatment with cyclohexane vapor results in a more hydrophobic surface, as demonstrated by water contact angle and XPS measurements. The length of the side chains plays a role in determining contact angle and compositional changes; for the samples studied, MBBPs with longer PEG side chains exhibited larger contact angle and compositional changes. Additionally, bottlebrush polymer films can be stabilized by addition of a bifunctional benzophenone cross-linker. This work demonstrates that bottlebrush polymers enable the preparation of stimuli-responsive, "brush-like" surface coatings using conventional solution processing methods.

EXPERIMENTAL SECTION

Materials. All reagents and solvents were purchased from Aldrich or VWR and were used as received unless otherwise noted. 2,2′-Azobis(2-methylpropionitrile) (AIBN) was purified by recrystallization in methanol. Styrene was passed through aluminum oxide column to remove inhibitors before use. Anhydrous dichloromethane (DCM) was dried over molecular sieves (4 Å) before use. *exo*-7-Oxabicyclo-[2.2.1]hept-5-ene-2,3-dicarboxylic anhydride,[63] 4-(2-hydroxyethyl)-10-oxa-4-azatricyclo[5.2.1.02,6]dec-8-ene-3,5-dione,[64] modified Grubb's catalyst $(H_2IMes)(pyr)_2(Cl)_2RuCHPh$,[65] and the bifunctional benzophenone molecule bis(3-benzoyl)benzoic acid ethylene glycol[51] were synthesized as previously reported. 2K and 5K azide-functionalized PEG were purchased from Nanocs.

N-(Hydroxypentanyl)-cis-5-norbornene-exo-2,3-dicarboximide. The synthetic procedure is a slightly modified from a previous report.[49] A round-bottom flask was charged with *cis*-5-norbornene-*exo*-2,3-dicarboxylic anhydride (0.95 g, 5.8 mmol) and 5-amino-1-pentanol (0.60 g, 5.8 mmol). Toluene (20 mL) and triethylamine (80 μL, 0.58 mmol) were added to the flask, and the reactor was refluxed at 125 °C with a Dean−Stark trap attached. After reacting for at least 4 h, the reaction was cooled down, and the solvent was removed by rotary evaporation. The resulting light yellow oil was redissolved in 20 mL of DCM and extracted with brine (10 mL) and then HCl (10 mL). The organic layer was dried by adding $MgSO_4$, and the resulting solution was concentrated under vacuum (1.40 g, 96% yield). ^{1}H NMR (400 MHz, $CDCl_3$, ppm): δ 6.27 (2H, CHC$\underline{H}$=C$\underline{H}$CH), 3.62 (2H, $CH_2C\underline{H}_2OH$), 3.44 (2H, $NC\underline{H}_2CH_2$), 3.27 (2H, CHC$\underline{H}$CH) 2.65 (2H, CHC$\underline{H}$CO), 1.49−1.56 (5H, $CH_2C\underline{H}_2C\underline{H}_2CH_2$; $CHC\underline{H}_2CH$), and 1.20−1.28 (3H, $CH_2C\underline{H}_2CH_2OH$; $CHC\underline{H}_2CH$).

N-(Pentynoylhexanyl)-cis-5-norbornene-exo-2,3-dicarboximide (1). The synthetic procedure is a slightly modified from a previous report.[49] *N*-(Hydroxypentanyl)-*cis*-5-norbornene-*exo*-2,3-dicarboximide (0.62 g, 2.5 mmol), 5-hexynoic acid (0.28 g, 2.5 mmol), and *N*, *N*′-dicyclohexylcarbodiimide (DCC) (0.62 g, 3.0 mmol) were dissolved in 10 mL of DCM and cooled in an ice bath. 4-(Dimethylamino)pyridine (DMAP) (0.10 g, 0.82 mmol) was then added. The reaction was stirred at 0 °C for 5 min and then allowed to come to room temperature, while stirring overnight. The organic layer was washed with water (2 × 10 mL) and brine (10 mL) and then dried with $MgSO_4$. The final product was purified with silica gel chromatography to obtain a light yellow oil (0.72 g, 84% yield). ^{1}H NMR (400 MHz, $CDCl_3$): δ and 6.28 (2H, CHC$\underline{H}$=C$\underline{H}$CH), 4.06 (2H, CH2C$\underline{H}_2$O), 3.46 (2H, $NC\underline{H}_2$CH2), 3.27 (2H, CHC$\underline{H}$CH), 2.67 (2H, CHC$\underline{H}$CO), 2.17−2.56 (4H, $COC\underline{H}_2C\underline{H}_2CH_2$), 1.98 (1H, CC$\underline{H}$), 1.50−1.55 (5H, $CH_2C\underline{H}_2C\underline{H}_2CH_2$; $CHC\underline{H}_2CH$), 1.18−1.45 (10H, norbornene spacer).

NB-PEG2K and NB-PEG 5K. PEG-azide (1 g) and *N*-(pentynoylhexanyl)-*cis*-5-norbornene-*exo*-2,3-dicarboximide (1 equiv to prepolymer end group) were dissolved in anhydrous *N,N*-dimethylformamide and purged by bubbling nitrogen through the solution for 30 min. Cu(I)Br was then added before adding a 1/9 v/v mixture of pyridine/toluene which was separately purged with nitrogen. The reaction was heated to

dx.doi.org/10.1021/ma301046n | *Macromolecules* 2012, 45, 7118−7127

50 °C and allowed to proceed overnight. The produce was passed through a basic alumina column to remove copper catalyst, concentrated under reduced pressure, and precipitated in cold diethyl ether to obtain a white powder. The product was dried under vacuum.

NB-PEG2K (0.99 g, 86% yield). ^{1}H NMR (400 MHz, $CDCl_3$): δ 7.50 (1H, C=C$\underline{H}$N), 6.29 (2H, CHC$\underline{H}$=C$\underline{H}$CH), 4.05 (2H, $CH_2C\underline{H}_2CO$), 3.50−3.90 (209H ($C\underline{H}_2C\underline{H}_2O)_n$), 3.48 (3H, $CH_2OC\underline{H}_3$), 1.2−1.7 (3H, $CH_2C\underline{H}_2CH_2OH$; CHC$\underline{H}_2$CH).

NB-PEG 5K (0.95 g, 88% yield). ^{1}H NMR (400 MHz, $CDCl_3$): δ 7.50 (1H, C=C$\underline{H}$N), 6.29 (2H, CHC$\underline{H}$=C$\underline{H}$CH), 4.05 (2H, $CH_2C\underline{H}_2CO$), 3.50−3.90 (509H ($C\underline{H}_2C\underline{H}_2O)_n$), 3.48 (3H, $CH_2OC\underline{H}_3$), 1.2−1.7 (3H, $CH_2C\underline{H}_2CH_2OH$; CHC$\underline{H}_2$CH).

Norbornene-Functionalized Chain-Transfer Agent (NB-CTA), N-(Pentynoyl-2-(dodecylthiocarbonothioylthio)-2-methylpropanyl)-cis-5-norbornene-exo-2,3-dicarboximide (2). 4-(2-Hydroxyethyl)-10-oxa-4-azatricyclo[5.2.1.02,6]dec-8-ene-3,5-dione (1.43 g, 6.85 mmol), 2-(dodecylthiocarbonothioylthio)-2-methylpropionic acid (2.50 g, 6.85 mmol), and *N,N′*-dicyclohexylcarbodiimide (1.61 g, 7.82 mmol) were dissolved in anhydrous dichloromethane (60 mL) and allowed to stir at 0 °C for 30 min. A solution of 4-(dimethylamino)pyridine in anhydrous DCM (5 mL, 0.65 mmol) was added dropwise. The reaction was stirred at 0 °C for 5 min and then allowed to come to room temperature while stirring overnight. The product was concentrated under reduced pressure and recrystallized in ethyl acetate/hexanes (1:4) solvent mixture. Crystals were collected by vacuum filtration and dried under vacuum (1.57 g, 40% yield). ^{1}H NMR (400 MHz, $CDCl_3$, ppm) (see Supporting Information Figure S1): δ 6.52 (2H, CHC$\underline{H}$=C$\underline{H}$CH), 5.29 (2H, CHC$\underline{H}$OCH), 4.22 (2H, $CH_2C\underline{H}_2O$), 3.77 (2H, $NC\underline{H}_2CH_2$), 3.2 (2H, $SC\underline{H}_2(CH_2)_{10}$), 2.89 (2H, CHC$\underline{H}$CCH), 1.66 (6H, $C(C\underline{H}_3)_2$), 1.29 (20H, $CH_2(C\underline{H}_2)_{10}CH_3$), 0.90 (3H, $CH_2C\underline{H}_3$).

Synthesis of NB-PS Macromonomers. NB-PS6K and NB-PS3K were prepared via reversible addition−fragmentation chain transfer (RAFT) polymerization. For the synthesis of NB-PS6K, styrene (4.84 g, 46.5 mmol), NB-CTA (101.40 mg, 0.182 mmol), and AIBN (3.40 mg, 1.82×10^{-2} mmol) were mixed in a 100 mL RBF, and the solution was purged by bubbling the nitrogen through the solution for 30 min. The polymerization was initiated by raising the temperature to 65 °C. After 11 h, the reaction flask was removed from heat, and the polymer was recovered by precipitation in methanol. For the synthesis of NB-PS3K, styrene (23.62 g, 227.1 mmol), NB-CTA (0.525 g, 0.917 mmol), and AIBN (0.197 mg, 1.20×10^{-3} mmol) were mixed in a 100 mL RBF, and the solution was purged by bubbling the nitrogen through the solution for 30 min. The polymerization was initiated by raising the temperature to 50 °C. After 5 days, the reaction flask was removed from heat and quenched by immersing in liquid N_2, and the polymer was recovered by precipitation in methanol

NB-PS6K (0.75 g, 67% yield, based on the conversion of styrene). ^{1}H NMR (400 MHz, $CDCl_3$, ppm): δ 6.30−7.25 (317H, styrenyl protons), 6.45 (2H, CHC$\underline{H}$=C$\underline{H}$CH) 5.20 (2H, CHCOC$\underline{H}$CH), 3.62 (2H, $CH_2C\underline{H}_2O$), 3.49 (2H, $NC\underline{H}_2CH_2$), 3.25 (2H, $SC\underline{H}_2(CH_2)_{10}$), 2.78 (2H, CHC$\underline{H}$CCH), 1.52 (6H, $C(C\underline{H}_3)_2$), 1.15−2.15 (127H, PS chain backbone protons), 1.26 (20H, $CH_2(C\underline{H}_2)_{10}CH_3$),0.88 (3H, $CH_2C\underline{H}_3$).

NB-PS3K (1.68 g, 61% yield, based on the conversion of styrene). ^{1}H NMR (400 MHz, $CDCl_3$, ppm): δ 6.30−7.25 (163H, styrenyl protons), 6.45 (2H, CHC$\underline{H}$=C$\underline{H}$CH) 5.20 (2H, CHCOC$\underline{H}$CH), 3.62 (2H, $CH_2C\underline{H}_2O$), 3.49 (2H, $NC\underline{H}_2CH_2$), 3.25 (2H, $SC\underline{H}_2(CH_2)_{10}$), 2.78 (2H, CHC$\underline{H}$CCH), 1.52 (6H, $C(C\underline{H}_3)_2$), 1.15−2.15 (65H, PS chain backbone protons), 1.26 (20H, $CH_2(C\underline{H}_2)_{10}CH_3$),0.88 (3H, $CH_2C\underline{H}_3$).

Synthesis of Mixed Bottlebrush Polymers through ROMP. MBBPs were prepared by ROMP using $(H_2IMes)(pyr)_2(Cl)_2RuCHPh$. The macromonomers were added to a dry, 25 mL round-bottom flask charged with a stir bar. The flask was then degassed with three pump−purge cycles, and the desired amount of degassed, anhydrous THF (total macromonomer concentration was 0.02−0.05 M) was added. $(H_2IMes)(pyr)_2(Cl)_2RuCHPh$ was dissolved in degassed, anhydrous THF in a separate flask. The catalyst solution was transferred to the reaction flask containing macromonomers via cannula to initiate the polymerization and stirred at room temperature for at least 1 h. The reaction was quenched by addition of ethyl vinyl ether after completion. The product was collected by precipitation in methanol or diethyl ether and dried under vacuum.

P(NB-PS6K-m-NB-PEG5K) (precipitated in methanol, 93% yield). M_w (GPC): 307 kg/mol, dn/dc = 0.0880, PDI = 1.13, DP (NMR) = 51. ^{1}H NMR (400 MHz, $CDCl_3$), δ (ppm): 6.36−7.50 (7630 H; styrenyl protons), 4.95 −5.90 (102 H; —C$\underline{H}$=C$\underline{H}$—), 3.4−3.89 (12852 H, PEG side-chain protons), 1.15−2.15 (4581H; PS side-chain protons).

P(NB-PS6K-m-NB-PEG2K) (precipitated in methanol, 90% yield). M_w (GPC): 302 kg/mol, dn/dc = 0.0880, PDI = 1.17, DP (NMR) = 69. ^{1}H NMR (400 MHz, $CDCl_3$), δ (ppm): 6.36−7.50 (10324 H; styrenyl protons), 4.95 −5.90 (138 H; —C$\underline{H}$=C$\underline{H}$—), 3.4−3.89 (7970 H, PEG chain backbone protons), 1.15−2.15 (6194 H; PS side-chain backbone protons).

P(NB-PS3K-m-NB-PEG2K)-1 (precipitated in diethyl ether, 84% yield). M_w (GPC): 165 kg/mol, dn/dc = 0.0870, PDI = 1.22, DP (NMR) = 58. ^{1}H NMR (400 MHz, $CDCl_3$), δ (ppm): 6.36−7.50 (4871H; styrenyl protons), 4.95 −5.90 (116 H; —C$\underline{H}$=C$\underline{H}$—), 3.4−3.89 (6457H, PEG side-chain protons), 1.15−2.15 (2923H; PS side-chain protons).

P(NB-PS3K-m-NB-PEG2K)-2 (precipitated in methanol, 87% yield). M_w (GPC): 302 kg/mol, dn/dc = 0.134, PDI = 1.38, DP (NMR) = 30. ^{1}H NMR (400 MHz, $CDCl_3$), δ (ppm): 6.36−7.50 (3080H; styrenyl protons), 4.95 −5.90 (60H; —C$\underline{H}$=C$\underline{H}$—), 3.4−3.89 (2614H, PEG side-chain protons), 1.15−2.15 (1848H; PS side-chain protons).

P(NB-PS3K-m-NB-PEG5K) (precipitated in diethyl ether, 89% yield). M_w (GPC): 132 kg/mol, dn/dc = 0.0813, PDI = 1.15, DP (NMR) = 29. ^{1}H NMR (400 MHz, $CDCl_3$), δ (ppm): 6.36−7.50 (2495H; styrenyl protons), 4.95 −5.90 (58H; —C$\underline{H}$=C$\underline{H}$—), 3.4−3.89 (13920H, PEG side-chain protons), 1.15−2.15 (1497H; PS side-chain protons).

P(NB-PS6K) (precipitated in methanol, 91% yield). M_w (GPC): 207 kg/mol, dn/dc = 0.158, PDI = 1.79, DP (NMR) = 33. ^{1}H NMR (400 MHz, $CDCl_3$), δ (ppm): 6.36−7.50 (10461H; styrenyl protons), 4.95 −5.90 (66H; —C$\underline{H}$=C$\underline{H}$—), 1.15−2.15 (4191H; PS side-chain protons).

P(NB-PS3K) (precipitate in methanol, 90% yield, based on the ROMP conversion). M_w (GPC): 207 kg/mol, dn/dc = 0.150, PDI = 107, DP (NMR) = 21. ^{1}H NMR (400 MHz, $CDCl_3$), δ (ppm): 6.36−7.50 (3423H; styrenyl protons), 4.95 −5.90 (42H; —C$\underline{H}$=C$\underline{H}$—), 1.15−2.15 (1365H; PS side-chain protons).

P(NB-PEG5K) (precipitated in diethyl ether, 90% yield). M_w (GPC): 59.6 kg/mol, dn/dc = 0.030, PDI = 1.07, DP (NMR) = 35. ^{1}H NMR (400 MHz, $CDCl_3$), δ (ppm): 4.95 −5.90 (70H; —C$\underline{H}$=C$\underline{H}$—), 3.4−3.89 (17815H, PEG side-chain protons).

P(NB-PEG2K) (precipitated in diethyl ether, 86% yield). M_w (GPC): 59.6 kg/mol, dn/dc = 0.030, PDI = 1.07, DP (NMR) = 25. ^{1}H NMR (400 MHz, $CDCl_3$), δ (ppm): 4.95 −5.90 (50H; —C$\underline{H}$=C$\underline{H}$—), 3.4−3.89 (5500H, PEG side-chain protons).

Preparation of MBBPs Films on ITO Glass. All contact angle, AFM, and XPS measurements reported were carried out on films prepared on ITO. Images shown on silicon are only for visualization of the films on a reflective surface. To prepare the polymer films, ITO glass substrates were immersed in each of the following solvents and sonicated for 60 min: 2% solution of basic cleaning solution Hellmanex in DI water, pure DI water, and isopropyl alcohol. The substrates were dried by under stream of compressed air and then under vacuum. Next, a MBBPs solution in chloroform (20 mg/mL) was prepared by stirring for 30 min before filtering using a 0.45 μm syringe filter. The filtered solution was then spin-cast onto the freshly cleaned ITO surfaces at a spin rate of 1500 rpm for 30 s and then 300 rpm for an additional 30 s. For solvent treatment, freshly prepared MBBPs film samples were dried under vacuum for 30 min and then placed in a sealed chamber with either methanol or cyclohexane under reduced pressure (−10 mmHg) and at room temperature overnight. After solvent-treatment, samples were removed from the sealed chamber and immediately dried under a flow of nitrogen before

dx.doi.org/10.1021/ma301046n | *Macromolecules* 2012, 45, 7118−7127

placing the film samples under vacuum overnight to remove residual solvents before testing.

Instrumentation. *Gel-Permeation Chromatography (GPC).* Molecular weights and polydispersities were obtained using an Agilent 1200 module equipped with three PSS SDV columns in series (100, 1000, and 10000 Å pore sizes), an Agilent variable wavelength UV/vis detector, a Wyatt Technology HELEOS II multiangle laser light scattering (MALLS) detector (λ = 658 nm), and a Wyatt Technology Optilab reX RI detector. This system enables SEC with simultaneous refractive index (SEC-RI), UV/vis (SEC-UV/vis), and MALLS detection. THF was used as the mobile phase at a flow rate of 1 mL/min at 40 °C.

Nuclear Magnetic Resonance Spectroscopy (NMR). Hydrogen NMR (^{1}H NMR) spectra were recorded using tetramethylsilane as internal standard in $CDCl_3$ on a 400 MHz Bruker multinuclear spectrometer. Samples were placed in 5 mm o.d. tubes with the concentration of 20 mg/mL.

Atomic Force Microscopy (AFM). AFM images were obtained with a Veeco Nanoscope V scanning probe controller in tapping mode in air at room temperature using silicon tips (resonance requency = 270–330 kHz and tip radius of curvature <10 nm).

Contact Angle Measurements. Static contact angle measurements of DI water on MBBPs thin films were carried out using a CAM 200 optical contact angle meter (KSV instruments, Monroe, CT) at ambient conditions. Water contact angles were measured after allowing the water droplet equilibrate on the surface for 180 s. Measurements were repeated on at least three substrates for each sample and at least on two different spots per substrate. The final reported values given represent an average of at least six measurements. All contact angle measurements were carried out on films on an ITO substrate.

X-ray Photoelectron Spectroscopy (XPS, PHI Quantera SXM). XPS was performed using monochromatic aluminum Kα X-rays. The incident angle of the beam to the sample is 45°. XPS data were analyzed with the MultiPak software. The samples were prepared by spin-casting solutions onto ITO substrates.

Grazing-Incidence Small-Angle X-ray Scattering (GISAXS). GISAXS measurements were carried out on the undulator-based beamline X9 at the National Synchrotron Light Source at Brookhaven National Laboratory. The monochromator was adjusted to select a photon energy of 14 keV (wavelength 0.886 nm). A Kirkpatrick-Biaz mirror system was used to focus the beam at the sample position (approximately 100 μm wide by 60 μm tall). Samples were measured under vacuum (~40 Pa), and the instrument was calibrated using a silver behenate powder as a standard. Data processing was carried out using a Python script developed on the X9 beamline. All measurements were carried out at an incident angle of 0.15°, which was measured by reflectivity to be above the critical angle. All films were measured on ITO substrates.

■ ASSOCIATED CONTENT

Supporting Information

NMR spectra of NB-CTA and bottlebrush polymers, GPC traces of bottlebrush and mixed bottlebrush polymers, optical microscopy and AFM images of bottlebrush polymer films, and GISAXS data. This material is available free of charge via the Internet at http://pubs.acs.org.

■ AUTHOR INFORMATION

Corresponding Author

*E-mail: rafaelv@rice.edu.

Notes

The authors declare no competing financial interest.

■ ACKNOWLEDGMENTS

The work was supported by the Welch Foundation for Chemical Research (Grant No. C-1750), the ACS Petroleum Research Fund (52345-DN17), Louis and Peaches Owen, the NASA ICA program, and Rice University School of Engineering start-up funds. S.L.P. acknowledges support from the National Science Foundation Graduate Fellowship Program. We gratefully acknowledge Dr. Yan Xia for helpful discussions regarding the synthesis of bottlebrush polymers and Dr. Zhibin Cheng for assistance with bottblebrush polymer schematics. We acknowledge Kevin Yager for help with GISAXS measurements. This material is based upon work supported by the National Science Foundation under Grant No. 0940902. Research carried out in part at the Center for Functional Nanomaterials, Brookhaven National Laboratory, which is supported by the U.S. Department of Energy, Office of Basic Energy Sciences, under Contract No. DE-AC02-98CH10886.

■ REFERENCES

(1) Fredrickson, G. H. *Macromolecules* **1993**, *26* (11), 2825–2831.
(2) Hsu, H.-P.; Paul, W.; Binder, K. *Macromol. Symp.* **2007**, *252* (1), 58–67.
(3) Zhang, B.; Gröhn, F.; Pedersen, J. S.; Fischer, K.; Schmidt, M. *Macromolecules* **2006**, *39* (24), 8440–8450.
(4) Rathgeber, S.; Pakula, T.; Wilk, A.; Matyjaszewski, K.; Beers, K. *J. Chem. Phys.* **2005**, *122*, 124904/1–124904/13.
(5) Sheiko, S. S.; Möller, M. *Chem. Rev.* **2001**, *101* (12), 4099–4124.
(6) Lee, S.; Spencer, N. D. *Science* **2008**, *319* (5863), 575–576.
(7) Runge, M. B.; Bowden, N. B. *J. Am. Chem. Soc.* **2007**, *129* (34), 10551–10560.
(8) Johnson, J. A.; Lu, Y. Y.; Burts, A. O.; Xia, Y.; Durrell, A. C.; Tirrell, D. A.; Grubbs, R. H. *Macromolecules* **2010**, *43* (24), 10326–10335.
(9) Li, Z.; Ma, J.; Cheng, C.; Zhang, K.; Wooley, K. L. *Macromolecules* **2010**, *43* (3), 1182–1184.
(10) Huang, K.; Rzayev, J. *J. Am. Chem. Soc.* **2009**, *131* (19), 6880–6885.
(11) Brittain, W. J.; Minko, S. *J. Polym. Sci., Part A: Polym. Chem.* **2007**, *45* (16), 3505–3512.
(12) Krishnan, S.; Weinman, C. J.; Ober, C. K. *J. Mater. Chem.* **2008**, *18* (29), 3405–3413.
(13) Rosenhahn, A.; Schilp, S.; Kreuzer, H. J.; Grunze, M. *Phys. Chem. Chem. Phys.* **2010**, *12* (17), 4275–4286.
(14) Howarter, J. A.; Youngblood, J. P. *Adv. Mater.* **2007**, *19* (22), 3838–3843.
(15) Chen, T.; Ferris, R.; Zhang, J.; Ducker, R.; Zauscher, S. *Prog. Polym. Sci.* **2010**, *35* (1–2), 94–112.
(16) Stuart, M. A. C.; Huck, W. T. S.; Genzer, J.; Muller, M.; Ober, C.; Stamm, M.; Sukhorukov, G. B.; Szleifer, I.; Tsukruk, V. V.; Urban, M.; Winnik, F.; Zauscher, S.; Luzinov, I.; Minko, S. *Nat. Mater.* **2010**, *9* (2), 101–113.
(17) Nath, N.; Chilkoti, A. *Adv. Mater.* **2002**, *14* (17), 1243–1247.
(18) Alonzo, J.; Chen, J.; Messman, J.; Yu, X.; Hong, K.; Deng, S.; Swader, O.; Dadmun, M.; Ankner, J. F.; Britt, P.; Mays, J. W.; Malagoli, M.; Sumpter, B. G.; Brédas, J.-L.; Kilbey, S. M. *Chem. Mater.* **2011**, *23* (19), 4367–4374.
(19) Sekovskyy, V.; Khanduyeva, N.; Komber, H.; Oertel, U.; Stamm, M.; Kuckling, D.; Kiriy, A. *J. Am. Chem. Soc.* **2007**, *129*, 6626–6632.
(20) Ayres, J. R. *J. Appl. Phys.* **1993**, *74* (3), 1787–1792.
(21) Bünsow, J.; Kelby, T. S.; Huck, W. T. S. *Acc. Chem. Res.* **2010**, *43* (3), 466–474.
(22) Matyjaszewski, K.; Dong, H.; Jakubowski, W.; Pietrasik, J.; Kusumo, A. *Langmuir* **2007**, *23* (8), 4528–4531.
(23) Barbey, R. l.; Lavanant, L.; Paripovic, D.; Schüwer, N.; Sugnaux, C.; Tugulu, S.; Klok, H.-A. *Chem. Rev.* **2009**, *109* (11), 5437–5527.
(24) Mansky, P.; Liu, Y.; Huang, E.; Russell, T. P.; Hawker, C. *Science* **1997**, *275* (5305), 1458–1460.
(25) Zhao, B.; Haasch, R. T.; MacLaren, S. *J. Am. Chem. Soc.* **2004**, *126* (19), 6124–6134.

(26) Sidorenko, A.; Minko, S.; Schenk-Meuser, K.; Duschner, H.; Stamm, M. *Langmuir* **1999**, *15* (24), 8349−8355.
(27) Estillore, N. C.; Advincula, R. C. *Langmuir* **2011**, *27* (10), 5997−6008.
(28) Granville, A. M.; Boyes, S. G.; Akgun, B.; Foster, M. D.; Brittain, W. J. *Macromolecules* **2004**, *37* (8), 2790−2796.
(29) Lee, H.-i.; Pietrasik, J.; Sheiko, S. S.; Matyjaszewski, K. *Prog. Polym. Sci.* **2010**, *35* (1−2), 24−44.
(30) Börner, H. G.; Beers, K.; Matyjaszewski, K.; Sheiko, S. S.; Möller, M. *Macromolecules* **2001**, *34* (13), 4375−4383.
(31) Cheng, G.; Böker, A.; Zhang, M.; Krausch, G.; Müller, A. H. E. *Macromolecules* **2001**, *34* (20), 6883−6888.
(32) Kriegel, R. M.; Rees, W. S.; Weck, M. *Macromolecules* **2004**, *37* (17), 6644−6649.
(33) Runge, M. B.; Dutta, S.; Bowden, N. B. *Macromolecules* **2006**, *39* (2), 498−508.
(34) Beers, K. L.; Gaynor, S. G.; Matyjaszewski, K.; Sheiko, S. S.; Moller, M. *Macromolecules* **1998**, *31* (26), 9413−9415.
(35) Huang, K.; Canterbury, D. P.; Rzayev, J. *Macromolecules* **2010**, *43* (16), 6632−6638.
(36) Rzayev, J. *Macromolecules* **2009**, *42* (6), 2135−2141.
(37) Xie, M.; Dang, J.; Han, H.; Wang, W.; Liu, J.; He, X.; Zhang, Y. *Macromolecules* **2008**, *41* (23), 9004−9010.
(38) Yamamoto, S.-i.; Pietrasik, J.; Matyjaszewski, K. *Macromolecules* **2007**, *40* (26), 9348−9353.
(39) Bolton, J.; Bailey, T. S.; Rzayev, J. *Nano Lett.* **2011**, *11* (3), 998−1001.
(40) Yamada, K.; Miyazaki, M.; Ohno, K.; Fukuda, T.; Minoda, M. *Macromolecules* **1998**, *32* (2), 290−293.
(41) Dziezok, P.; Fischer, K.; Schmidt, M.; Sheiko, S. S.; Möller, M. *Angew. Chem., Int. Ed.* **1997**, *36* (24), 2812−2815.
(42) Wintermantel, M.; Gerle, M.; Fischer, K.; Schmidt, M.; Wataoka, I.; Urakawa, H.; Kajiwara, K.; Tsukahara, Y. *Macromolecules* **1996**, *29* (3), 978−983.
(43) Wintermantel, M.; Fischer, K.; Gerle, M.; Ries, R.; Schmidt, M.; Kajiwara, K.; Urakawa, H.; Wataoka, I. *Angew. Chem., Int. Ed.* **1995**, *34* (13−14), 1472−1474.
(44) Tsukahara, Y.; Ohta, Y.; Senoo, K. *Polymer* **1995**, *36* (17), 3413−3416.
(45) Tsukahara, Y.; Kohjiya, S.; Tsutsumi, K.; Okamoto, Y. *Macromolecules* **1994**, *27* (6), 1662−1664.
(46) Xia, Y.; Olsen, B. D.; Kornfield, J. A.; Grubbs, R. H. *J. Am. Chem. Soc.* **2009**, *131* (51), 18525−18532.
(47) Jha, S.; Dutta, S.; Bowden, N. B. *Macromolecules* **2004**, *37* (12), 4365−4374.
(48) Runge, M. B.; Yoo, J.; Bowden, N. B. *Macromol. Rapid Commun.* **2009**, *30* (16), 1392−1398.
(49) Xia, Y.; Kornfield, J. A.; Grubbs, R. H. *Macromolecules* **2009**, *42* (11), 3761−3766.
(50) Li, Z.; Zhang, K.; Ma, J.; Cheng, C.; Wooley, K. L. *J. Polym. Sci., Part A: Polym. Chem.* **2009**, *47*, 5557.
(51) Carroll, G. T.; Sojka, M. E.; Lei, X.; Turro, N. J.; Koberstein, J. T. *Langmuir* **2006**, *22* (18), 7748−7754.
(52) Soga, K. G.; Zuckermann, M. J.; Guo, H. *Macromolecules* **1996**, *29* (6), 1998−2005.
(53) Motornov, M.; Sheparovych, R.; Katz, E.; Minko, S. *ACS Nano* **2008**, *2* (1), 41−52.
(54) Ayres, N.; Boyes, S. G.; Brittain, W. J. *Langmuir* **2006**, *23* (1), 182−189.
(55) Zhao, B.; Brittian, W. J. *J. Am. Chem. Soc.* **1999**, *121*, 3557−3558.
(56) Rowe, M. D.; Hammer, B. A. G.; Boyes, S. G. *Macromolecules* **2008**, *41* (12), 4147−4157.
(57) Drumheller, P. D.; Hubbell, J. A. *J. Biomed. Mater. Res.* **1995**, *29* (2), 207−215.
(58) Ostaci, R.-V.; Damiron, D.; Grohens, Y.; Léger, L.; Drockenmuller, E. *Langmuir* **2009**, *26* (2), 1304−1310.
(59) Zdyrko, B.; Klep, V.; Luzinov, I. *Langmuir* **2003**, *19* (24), 10179−10187.
(60) Xia, N.; Hu, Y.; Grainger, D. W.; Castner, D. G. *Langmuir* **2002**, *18* (8), 3255−3262.
(61) Lee, S.-W.; Laibinis, P. E. *Biomaterials* **1998**, *19* (18), 1669−1675.
(62) Groll, J.; Fiedler, J.; Engelhard, E.; Ameringer, T.; Tugulu, S.; Klok, H.-A.; Brenner, R. E.; Moeller, M. *J. Biomed. Mater. Res., Part A* **2005**, *74A* (4), 607−617.
(63) France, M. B.; Alty, L. T.; Earl, T. M. *J. Chem. Educ.* **1999**, *76* (5), 659.
(64) Mantovani, G.; Lecolley, F.; Tao, L.; Haddleton, D. M.; Clerx, J.; Cornelissen, J. J. L. M.; Velonia, K. *J. Am. Chem. Soc.* **2005**, *127* (9), 2966−2973.
(65) Sanford, M. S.; Love, J. A.; Grubbs, R. H. *Organometallics* **2001**, *20* (25), 5314−5318.